Singular behavior at the edge of Laughlin states

T. Can,[1] P. J. Forrester,[2] G. Téllez,[3] and P. Wiegmann[1]
[1]*Department of Physics, University of Chicago, 929 57th St, Chicago, Illinois 60637, USA*
[2]*Department of Mathematics and Statistics, The University of Melbourne, Victoria 3010, Australia*
[3]*Departamento de Física, Universidad de Los Andes, Bogotá, Colombia*
(Received 6 August 2013; revised manuscript received 27 May 2014; published 30 June 2014)

A distinguishing feature of fractional quantum Hall (FQH) states is a singular behavior of equilibrium densities at boundaries. In contrast to states at integer filling fraction, such quantum liquids posses an additional dipole moment localized near edges. It enters observable quantities such as universal dispersion of edge states and Lorentz shear stress. For a Laughlin state, this behavior is seen as a peak, or overshoot, in the single-particle density near the edge, reflecting a general tendency of electrons in FQH states to cluster near edges. We compute the singular edge behavior of the one-particle density by a perturbative expansion carried out around a completely filled Landau level. This correction is shown to fully capture the dipole moment and the major features of the overshoot observed numerically. Furthermore, it exhibits the Stokes phenomenon with the Stokes line at the boundary of the droplet, decaying like a Gaussian inside and outside the liquid with different decay lengths. In the limit of vanishing magnetic length, the shape of the overshoot is a singular double layer with a capacity that is a universal function of the filling fraction. Finally, we derive the edge dipole moment of Pfaffian FQH states. The result suggests an explicit connection between the magnitude of the dipole moment and the bulk odd viscosity.

DOI: 10.1103/PhysRevB.89.235137 PACS number(s): 73.43.−f, 05.20.−y

I. INTRODUCTION

One of the distinct features of fractional quantum Hall (FQH) states is the nonmonotonic behavior of static correlation functions at short distances. Such behavior has physical consequences. One of the most familiar is the magnetoroton minimum in the dispersion curve of the gapped collective excitations. This was first demonstrated for Laughlin states (states with the filling fraction equal to the inverse of an odd integer [1]) using a variational formula for the energy spectrum which involves the static structure factor of the FQH ground state [2]. The dip in the dispersion curve was attributed to a peak that occurs in the numerically computed static structure factor. Numerical studies show that this peak is followed by damped oscillatory features [3], already apparent in the $\nu = 1/3$ state [2]. That the magnetoroton minimum disappears for the integer quantum Hall (IQH) state can also be deduced directly from its static structure factor, which, in this case ($\nu = 1$) is a monotonically increasing function of momentum. The pair correlation function in coordinate space possesses the same structure as the static structure factor (the Fourier transform of the pair density correlation function). The pair correlation function oscillates as separation between points decreases, then rises up before vanishing at zero separation [2].

Similar, nonmonotonic behavior is seen in the one-particle density of FQH states, which displays a prominent peak, or "overshoot," at the edge [4]. This behavior has been observed numerically in the Laughlin states [5–8]. This is in stark contrast to the particle density of the IQH state, which monotonically decreases with distance from the center of mass, as seen in Fig. 1. Consequently, states with a fractional filling factor possess a dipole moment, as well as higher order moments, additional to the integer case and localized near the edge.

The overshoot in the one-particle density is seen to have noticeable physical consequences. Recently, it has been shown that the double layer is an essential ingredient in the theory of edge waves that supports fractionally charged edge solitons [9]. In the same paper, it was conjectured that in the limit of vanishing magnetic length the edge dipole moment is in fact a *double layer* with a capacity, which is a universal function of the filling fraction [9]. The universal properties of the edge dipole are also closely linked to the Lorentz shear stress, an intrinsic property of the bulk [10,11].

There is a very good reason to think that these two peaks, or overshoots, are closely related. Indeed, the pair correlation function in coordinate space is equivalent to the one-particle density around a hole, or puncture, which is effectively an edge with large curvature. Thus both features can be understood as a tendency of electrons in the FQH state to cluster at inner edges of the droplet. The overshoot in the density and pair correlation function should be understood as a key feature of the FQH state, one that is conspicuously absent in the IQH state.

While the significance of such edge singularities is now appreciated, an understanding of them has thus far relied almost entirely on numerics. Of the handful of analytic works in the literature, we refer to [12,13] for attempts to capture this behavior in the bulk pair correlation function and [14,15] in relation to the boundary overshoot.

The goal of this paper is to shed light on the density overshoot at the edge. We are primarily concerned with the analytical structure of the edge density. We find that the most reliable approach is to treat the inverse filling fraction $\nu^{-1} = \beta$ as a parameter in Laughlin's wave function and to expand the edge density about its known value for the completely filled Landau level $\beta = 1$ to first order in the perturbation variable $\beta - 1$. This approach has been successfully executed by Jancovici in Ref. [13] for the bulk pair correlation function. The leading correction is shown to herald the overshoot for the Laughlin states. Since the 2D one component plasma is not believed to have a phase transition in the domain of β relevant for FQH states, we assume the results near $\beta = 1$ can

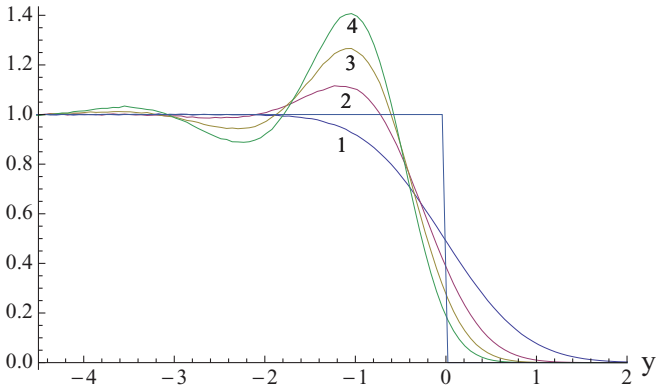

FIG. 1. (Color online) Density profile near the edge of the droplet $\rho_\beta(y)/\bar{\rho}$, labeled by the value of β (equal to the inverse filling fraction ν^{-1} for odd integer values). For reference, the support of the droplet is plotted as a step function. Data obtained by numerical simulation [16]. Distance y is measured in units of ℓ.

be adiabatically connected to the $\beta = 3,5,\ldots$, and specifically that the $\beta - 1$ term evolves smoothly into the overshoot seen in the Laughlin state. This argument is supported by numerical data.

The overshoot at the boundary and subsequent oscillatory features (not captured by the first order correction) extended toward the bulk of the droplet could be assigned to a tendency toward crystallization as β increases. The "crystallization" is more pronounced in the vicinity of the boundary.

In this paper, we focus on Laughlin states, and briefly discuss possible extensions to other FQH states. We expect more complicated FQH states also feature singular behavior on edges, and as a first step toward understanding their structure we compute the edge dipole moment for Pfaffian states. In Sec. II, we present our main results, the derivation of which is summarized in the subsequent sections. Further detailed derivations will be presented in an expanded companion paper [17].

II. NOTATION AND THE MAIN RESULTS

The Laughlin state of N particles on a cylinder of circumference L_x at the filling fraction $\nu = 1/\beta$ in the Landau gauge is [18]

$$\Psi_\beta(z_1,\ldots,z_N) = Z_N^{-1/2}\Delta^\beta \exp\left(-\pi\beta\bar{\rho}\sum_{i=1}^N y_i^2\right), \qquad (1)$$

where $z_i = x_i + iy_i$ is the coordinate on the cylinder, $\bar{\rho} = (2\pi\beta\ell_B^2)^{-1}$ is the mean density, $\ell_B = \sqrt{\hbar c/eB}$ is the magnetic length, Z_N is the normalization factor, and

$$\Delta = \prod_{i<j}\left(e^{i2\pi z_i/L_x} - e^{i2\pi z_j/L_x}\right).$$

We assume that $\ell = \sqrt{\beta}\ell_B$ is held constant, while varying β, so that the mean density $\bar{\rho} = (2\pi\ell^2)^{-1}$ is independent of β. Below, we set the units of length along the cylinder $\ell = 1$. In these units the mean density is $\bar{\rho} = (2\pi)^{-1}$.

We are interested in the one-particle density for a large number of particles,

$$\rho_\beta(y) = N\int |\Psi_\beta(z,z_2,\ldots,z_N)|^2 \prod_{i=2}^N dx_i dy_i. \qquad (2)$$

The square of the amplitude of the Laughlin wave function $|\Psi_\beta|^2$ can be seen as the Boltzmann weight of a 2D Coulomb plasma on a cylinder, with neutralizing uniform background charge in the rectangle

$$\mathcal{R} := \{0 \leqslant x \leqslant L_x, -\tau L_x \leqslant y \leqslant 0\},$$

where $\tau = N/(\bar{\rho}L_x^2)$ is an aspect ratio, and β acting as the inverse temperature. The plasma forms a droplet in $\mathcal{R}$ with approximately uniform density $\bar{\rho}$. The mean position of the center of the droplet is given by the exact sum rule:

$$\bar{y} = N^{-1}\int y\rho_\beta(y)dy = -\frac{L_x\tau}{2}\left(1 - \frac{1}{N}\right). \qquad (3)$$

Outside the droplet, the density decays as a Gaussian. We focus on the density near the right boundary at $y = 0$, sending the left boundary to negative infinity. This is accomplished by fixing $\bar{\rho}$, τ, y and sending $N \to \infty$. In this limit, the shape of the density is a universal (N, τ, and L_x independent) function of y. It depends continuously on β as a parameter. The particle density for different β, obtained via simulation, is plotted in Fig. 1. The density approaches $\bar{\rho}$ in the bulk.

For $\beta = 1$, the limiting shape of the density can be computed analytically from the exact finite N form [19] (see also the sentence below (14)), and we find

$$\rho_1(y) = \frac{\bar{\rho}}{2}\mathrm{erfc}(y) \approx \bar{\rho}\begin{cases}1 - (2\sqrt{\pi}|y|)^{-1}e^{-y^2}, & -y \gg 1,\\ (2\sqrt{\pi}|y|)^{-1}e^{-y^2}, & y \gg 1.\end{cases} \qquad (4)$$

We would like to emphasize the Stokes phenomena already seen in this simple case: the density is an entire function having analytically discontinuous asymptotes at different parts of the complex plane z.

Below [see Eq. (22)], we compute $\rho_\beta(y)$ to the leading order in $\beta - 1$, obtaining the exact functional form of

$$f(y) = \left[\frac{\partial\rho_\beta}{\bar{\rho}\partial\beta}\right]_{\beta=1}. \qquad (5)$$

The function $f(y)$ is an entire function. It shows a richer Stokes phenomena: at large $|y|$ inside and outside the droplet the density behaves as

$$f(y) = \frac{1}{2\sqrt{\pi}}\begin{cases}3^{5/2}\ y^{-3}e^{-y^2/3}, & -y \gg 1 \text{ (inside)},\\ -|y|\ e^{-y^2}, & y \gg 1 \text{ (outside)}.\end{cases} \qquad (6)$$

In fact, the leading large y asymptote outside the droplet is independently known for all β [17,20] up to the coefficient c_β. It is

$$\rho_\beta(y) \approx \bar{\rho}\,\frac{c_\beta}{\sqrt{2\pi}}(|y|\sqrt{2})^{-\beta}e^{-\beta y^2}. \qquad (7)$$

The leading order of the $\beta - 1$ expansion of the coefficient c_β is found to be

$$c_\beta \approx 1 + (\beta - 1)(1 - \mathbf{C})/2 + \mathcal{O}(\beta - 1)^2,$$

where $\mathbf{C}$ is the Euler-Mascheroni constant [17].

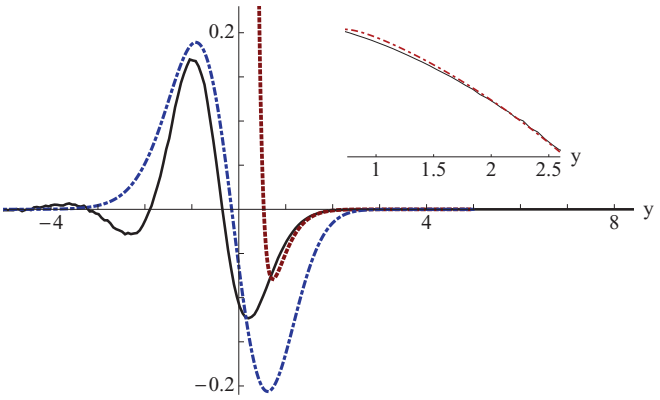

FIG. 2. (Color online) Comparison of the numerically computed $(\rho_\beta - \rho_1)/[\bar{\rho}(\beta-1)]$ (solid line) for the Laughlin state $\nu = \beta^{-1} = 1/3$, with the $\mathcal{O}(\beta-1)$ correction $f(y)$ (blue dash-dotted line), and its exterior asymptote Eq. (7) (red dashed line). The overshoot at the inner edge is captured well by $f(y)$. (Inset) Logarithmic-scale comparison of exterior asymptote to numerical data for the density. Distance is measured in units of ℓ.

The asymptotes of the correction to $\rho_1(y)$ given by $f(y)$ imply an overshoot at the edge if $\beta > 1$. This follows by observing that, when approaching from the inside of the droplet ($y < 0$), the correction is positive and rising, while approaching from the outside the correction is negative. A depletion of charge outside the droplet, and accumulation inside is thus implied. Since the total number of particles remains the same, this behavior yields the overshoot. Also, the asymmetry of the asymptotes suggests that the accumulation inside is larger than the depletion outside, indicating a shift of the boundary [where $f(y)$ vanishes] towards the interior.

A noticeable feature of the correction is the asymmetry of inside and outside behavior not seen in the integer case where $\rho_1(-y) = \bar{\rho} - \rho_1(y)$. Moreover, even deep inside the droplet the $\beta-1$ correction $\mathcal{O}(\exp(-y^2/3))$ dominates the $\beta = 1$ contribution $\mathcal{O}(\exp(-y^2))$. This signals that higher order $\beta-1$ corrections are even more relevant deep inside the droplet. They are responsible for oscillatory features evident in numerics.

The full function $f(y)$ is plotted in Fig. 2, where it is compared with both numerical data for the normalized difference $[\rho_\beta(y) - \rho_1(y)]/[\bar{\rho}(\beta-1)]$ at the filling fraction $\nu = 1/3$, as well as the exterior asymptote of this difference, which follows from Eq. (7) with $\beta = 3$ and the numerical approximation for c_β computed in Refs. [8] and [17]. We observe the function $f(y)$ captures well the overshoot at the inner boundary, as well as the gross overall features of the edge double layer. However, it misses the oscillatory features which arise inside the droplet, since as remarked in the previous paragraph, these are likely non-perturbative corrections in $\beta-1$. The exterior asymptote also shows good agreement with the numerics at distances from the edge of order ℓ. Therefore Eqs. (6) and (7) effectively capture the overshoot and approximately illustrate the edge double layer.

Thus, we see that deviations of ρ_β from ρ_1 and subsequently from the step function are localized to distances of a few magnetic lengths near the edge. In considering the limit of vanishing magnetic length, while keeping the area of the droplet $2\pi\beta\ell_B^2 N$ fixed, we see the function $f(y)$ collapses to the *double layer* conjectured in Ref. [9] (see also Refs. [14,15]). In original units,

$$\rho_\beta(y) - \rho_1(y) = \frac{(\beta-1)}{4\pi\beta}\delta'(y). \tag{8}$$

This formula succinctly describes the dipole moment per unit length along the edge

$$\int y[\rho_\beta(y) - \rho_1(y)]dy = -\frac{\beta-1}{4\pi\beta} \tag{9}$$

known independently [15] (see Sec. VII below). The dipole moment is completely captured by the $\beta-1$ expansion through the correction $f(y)$.

Higher moments

$$M_n \equiv \int_{-\infty}^{\infty} y^n f(y)dy$$

grow as $n!$. The odd moments can be obtained explicitly:

$$M_{2n+1} = -\frac{(2n+1)!}{4^n(n+1)!}\left(\frac{1}{2} + \sum_{k=1}^{n} R_k\right),$$
$$R_k = \frac{3^{k+1}(4k+5) + (2k^2+4k+1)}{16(k+2)(k+1)}. \tag{10}$$

Finally, in Sec. VIII, we compute the edge dipole moment per unit length for the Pfaffian states. The result further confirms the close connection between the dipole moment and the Lorentz shear stress alluded to in the introduction.

III. EDGE DENSITY AT $\beta = 1$

If $\beta = 1$ [19], the wave function (1) describes free fermions on the lowest Landau level. It is the Slater determinant

$$\Psi_1 = \det[\psi_{n-1}(z_i)]_{1\leqslant n,i\leqslant N}$$

of one-particle wave functions

$$\psi_n(z) = (L_x\sqrt{\pi})^{-1/2} e^{-\frac{1}{2}(y+p_n)^2} e^{ip_n x},$$

where $p_n = 2\pi n L_x^{-1}$, $n = 0,\ldots,N-1$. Consequently, the n-point function

$$g_1^{(n)} \equiv \frac{N!}{(N-n)!}\int |\Psi_1(z_1,\ldots,z_N)|^2 \prod_{i=n+1}^{N} d^2 z_i \tag{11}$$

is also a determinant (per Wick's theorem) $g_1^{(n)} = \det[K(z_i,z_j)]_{i,j=1,\ldots,n}$. Here,

$$K(z_1,z_2) = \sum_{n=0}^{N-1} \psi_n(z_1)\psi_n^*(z_2) \tag{12}$$

is the Fredholm kernel (projector) over the Landau level. We will use the Fourier modes of the kernel along the boundary:

$$K(z_1,z_2) = L_x^{-1}\sum_{n=0}^{N-1} K_{p_n}(y_1,y_2)e^{ip_n(x_1-x_2)}, \tag{13}$$

$$K_p(y_1,y_2) = \frac{1}{\sqrt{\pi}} e^{-\frac{1}{2}(y_1+p)^2} e^{-\frac{1}{2}(y_2+p)^2}. \tag{14}$$

In particular, for the density, we have

$$\rho_1(y) = L_x^{-1} \sum_p K_p(y,y).$$

The limiting shape of the density is given by (4).

IV. PERTURBATION EXPANSION IN $\beta - 1$

As β departs from 1, the wave function and correlation functions depart from the determinantal form. This can be viewed as an interaction between fermions. We can develop a perturbation expansion of the density around $\beta = 1$ by direct expansion of (2) in $\beta - 1$.

Defining the expectation value over free fermions $\langle \mathcal{A} \rangle = \int \Psi_1^* \mathcal{A} \Psi_1 \prod_{i=1}^N dx_i dy_i$, where $\mathcal{A}$ is a symmetric function of coordinates, we write the first correction to the unperturbed density $\rho_1(y)$ as

$$f(y) = -2\pi \left\langle \sum_i \delta^{(2)}(z - z_i) \left[\sum_{j>k} V(z_j, z_k) + \sum_j y_j^2 \right] \right\rangle_c , \tag{15}$$

where

$$V(z,z') = -\ln \left| e^{2\pi i z/L_x} - e^{2\pi i z'/L_x} \right|^2 . \tag{16}$$

The symbol $\langle ... \rangle_c$ stands for the connected part of the correlation function defined for two operators as $\langle AB \rangle_c = \langle AB \rangle - \langle A \rangle \langle B \rangle$. In this case, it involves one-, two-, and three-point correlation functions, which can be computed using Wick's theorem. The result is expressed through the two-body interaction potential

$$\varphi_1(z) = \int d^2 z' \rho_1(z') V(z,z') + y^2$$

and the two-body potential $V(z,z')$. We can write both contributions together by introducing a nonsymmetric potential

$$v(z_1, z_2) = -\varphi_1(z_1) + V(z_1, z_2). \tag{17}$$

The result reads

$$f(y) = 2\pi \int d^2 z' d^2 z'' K(z,z') K(z',z'') K(z'',z) \times [v(z,z') - v(z',z'')]. \tag{18}$$

We comment that perturbation theory around the integer filling factor could be carried out from the phenomenological Hamiltonian of the FQHE considered in Ref. [9]. We briefly describe it.

The Hilbert space of FQH states is comprised of functions $Q\Psi_1$, where $Q = Q_k(e^{2\pi i z_1/L_x}, \ldots, e^{2\pi i z_N/L_x}) e^{-\frac{k}{2}\sum_{i=1}^N y_i^2}$, and Q_k is a symmetric polynomial of the degree $k-1$. In particular, Laughlin's wave function corresponds to $k = \beta - 1$ and $Q_k = \Delta^{\beta-1}$. The operators acting in this space are symmetric functions of coordinates and derivatives. Their matrix elements are $\langle Q|\mathcal{A}|Q' \rangle = \int |\Psi_1|^2 Q \mathcal{A} Q' \prod_i dx_i dy_i$, where derivatives in $\mathcal{A}$ (if any) act to the right. Magnetic translation operators in this representation are

$$\mathrm{p}_i = \partial_{z_i} - (\beta - 1)\partial_{z_i} \left[y_i^2 + \sum_{j \neq i} V(z_i, z_j) \right].$$

Each operator annihilates the Laughlin state $\mathrm{p}_i \Psi_\beta = 0$.

The phenomenological Hamiltonian is constructed as a square of magnetic translations $H = \sum_i \mathrm{p}_i^\dagger \mathrm{p}_i$. Its spectrum is non-negative, with the Laughlin wave function as the zero energy ground state. The interaction is explicit in the Hamiltonian. The formula (15) could be obtained as the leading order of the perturbation expansion.

Further calculations are most conveniently done using Fourier modes. We write the potential as

$$v(z,z') = v_0(y,y') + \sum_{n=1}^{\infty} 2\cos(k_n(x'-x)) v_n(y-y'),$$

where

$$v_n(y) = \frac{2\pi}{L_x k_n} e^{-k_n|y|}, \quad v_0(y,y') = \frac{4\pi}{L_x} \min(y,y') - \varphi_1(y).$$

Then

$$f(y) = \frac{2\pi}{L_x} \sum_{n,m=0}^{N-1} \int dy' dy'' K_{p_n}(y,y') K_{p_m}(y',y'')) \times [K_{p_m}(y'',y) v_{|n-m|}(y,y') - K_{p_n}(y'',y) v_{|n-m|}(y',y'')]. \tag{19}$$

The integrals in y can be computed analytically. The result is expressed through the error function $\mathrm{erf}(y) = \frac{2}{\sqrt{\pi}} \int_0^y e^{-y'^2} dy'$, $\mathrm{erfc}(y) = 1 - \mathrm{erf}(y)$ and its antiderivative

$$F(y) = -y\,\mathrm{erfc}(y) + \frac{1}{\sqrt{\pi}} e^{-y^2}, \quad F'(y) = -\mathrm{erfc}(y).$$

We list the contributions of the zero and nonzero modes separately $f(y) = f^{(1)}(y) + f^{(2)}(y)$,

$$f^{(1)}(y) = 2\pi (y\rho_1)' + \frac{\pi}{2}\rho_1''(y) + \frac{1}{\sqrt{\pi}} \left(\frac{2\pi}{L_x} \right)^2 \times \sum_{0 \leqslant n \neq m < N} e^{-(y+p_n)^2} \left[F(y + p_m) - \sqrt{2} F\left(\frac{p_m - p_n}{\sqrt{2}} \right) \right], \tag{20}$$

$$f^{(2)}(y) = \frac{1}{\sqrt{\pi}} \left(\frac{2\pi}{L_x} \right)^2 \sum_{0 \leqslant n \neq m < N} \frac{e^{-(y+p_n)^2}}{p_n - p_m} \times \left[\mathrm{erf}(y + p_m) + \mathrm{erf}\left(\frac{p_n - p_m}{\sqrt{2}} \right) \right]. \tag{21}$$

This formula could be studied in various different large N limits, while y is of the order 1. One is the limit of the thin cylinder with the large aspect ratio $\tau \gg 1$, when the circumference L_x is comparable with the magnetic length. In this case electrons are crystallized all the way into the bulk [19,21,22]. The density is a nearly periodic function featuring N humps with a width of the magnetic length localized at $y_n = 2\pi n/L_x$. The contribution comes only from the zero mode (20). In this case, the correction we computed does not drastically change the profile away from $\beta = 1$.

However, for a cylinder with aspect ratio of order 1, the genuine 2D case, the distance between humps and the size of the humps are of the same order. The sums in (20) and (21)

must be replaced by integrals. This gives the limiting shape

$$f^{(1)}(y) = \frac{1}{2}\mathrm{erfc}(y) - \frac{y}{2\sqrt{\pi}}e^{-y^2} + \frac{1}{\sqrt{\pi}}\iint_y^\infty e^{-p^2}\left[F(p') - \sqrt{2}F\left(\frac{p'-p}{\sqrt{2}}\right)\right]dpdp',$$
$$f^{(2)}(y) = \frac{1}{\sqrt{\pi}}\iint_y^\infty \frac{e^{-p^2}}{p-p'}\left[\mathrm{erf}\,p' + \mathrm{erf}\left(\frac{p-p'}{\sqrt{2}}\right)\right]dpdp'. \quad (22)$$

The formulas are more transparent if we focus on the antisymmetric part of the correction $f_A(y) = \frac{1}{2}[f(y) - f(-y)]$. The result is more compact if one applies the differential operator $D = (\partial_y + 2y)\partial_y$ to the antisymmetric part. This operator annihilates the zero-order part of the density $D\rho_1 = 0$. After some tedious algebra we get

$$Df_A = \left(y^2 - \frac{1}{2}\right)\left(\mathrm{erf}\left(\frac{y}{\sqrt{3}}\right) - \mathrm{erf}(y)\right) + \frac{\sqrt{3}}{\sqrt{\pi}}ye^{-\frac{y^2}{3}}. \quad (23)$$

The odd moments (10) were computed from this formula.

V. ASYMPTOTES OF THE OVERSHOOT

These formulas are sufficient to compute the asymptotes of the overshoot at large $|y|$ (larger than magnetic length but smaller than the circumference of the boundary). They are summarized in Sec. II.

The asymptotes outside of the droplet are readily computable directly from the integrals (22). In this case, the integrals in (22) are suppressed by the factor e^{-p^2}. We reproduce the $\beta - 1$ expansion of the known asymptote (7) and obtain the $\beta - 1$ expansion of the previously unknown coefficient c_β [17].

Inside the droplet (23) indicates that the dominant term comes from $\mathrm{erf}(y/\sqrt{3})$ and the last term in (23). It is $\mathcal{O}(e^{-y^2/3})$ and therefore dominates other contributions of the order $\mathcal{O}(e^{-y^2})$. As a result, inside the droplet $f \approx 2f_A$. The asymptotes of f_A easily follow from (23). The result is presented in (6).

We also want to comment further on the emergence of the curious $e^{-y^2/3}$ asymptote only inside the droplet. A similar effect is seen in the $\beta - 1$ correction to the pair distribution function $g_\beta(r_1, r_2)$ deep inside the bulk where it depends only on the distance between the points. At $\beta = 1$ the pair correlation function is $g_1(r) = 1 - e^{-r^2/2}$ as it follows from (11) and (12). However, the correction computed in Ref. [13] has the asymptote $\sim r^{-2}\exp(-r^2/4)$. In that case, the appearance of the different exponent can be understood as necessarily following from the functional rule $g_\beta(r) = -e^{-r^2/2}g_\beta(ir)$ for the pair correlation function [23]. To the best of our knowledge, there is no analogous sum rule to explain the $\exp(-y^2/3)$ decay for the density. We expect that higher-order corrections show even slower decay, indicating the development of oscillations extended into the bulk. The apparent asymmetry between asymptotes inside and outside the droplet and a decay $\mathcal{O}(e^{-y^2/3})$ are perhaps the major analytic findings of the paper.

VI. SINGULAR DOUBLE LAYER

To capture the singular character of the edge, we consider the different limit when $\ell \to 0$. In this case, the limiting shape collapses to a singularity at the edge. Let us restore the magnetic length in the formulas (10), fix y and send magnetic length to zero. In the original coordinates, the moments

$$\int [\rho_\beta(y) - \rho_1(y)]y^n dy = (2\pi)^{-1}(\beta - 1)\ell^{n-1}M_n$$

are scaled as ℓ^{n-1}. In the limit $\ell \to 0$, the only moment that remains is the dimensionless dipole moment $M_1 = -1/2$. It is saturated by the double layer (8).

We want to emphasize that this is a fundamental feature of the Laughlin state that persists in the thermodynamic (large N) limit. In taking the limit of $N \to \infty$ and $\ell \to 0$, the droplet tends to a uniform density on a domain with a step-function support. However, the magnitude of the dipole moment per unit length along the boundary is a universal function of the filling fraction, and survives in the large N limit. Since the dipole moment is localized to distances $\mathcal{O}(\ell)$ near the edge, this gives rise to a singular double layer correction at the boundary of the droplet, which is *essential* to the physics of the FQH state.

VII. DIPOLE MOMENT FROM EXACT SUM RULE IN DISK GEOMETRY

Though we have specialized the preceding discussion to the case of a cylindrical geometry, the edge density derived above also follows from studying the Laughlin state in the disk geometry in local coordinates, and under the proper scaling limit, in which the droplet boundary appears approximately flat (vanishing geodesic curvature). This is discussed in great detail in the companion paper [17]. This universality of the edge density can be understood as arising from the finite correlation length in the bulk, wherein correlations show Gaussian decay over a characteristic distance on the order of the magnetic length. Thus, the shape of the droplet is invisible to the edge density, which is defined for distances from the boundary on the order or larger than ℓ, but much less than the droplet size.

In this section, we present an alternative derivation of the edge dipole moment from an exact sum rule for the droplet in the disk geometry. This was obtained in Ref. [15], and we repeat the arguments below. In the next section, we use this approach to compute the dipole moment of Pfaffian FQH ground-state wave functions.

To begin, we write the Laughlin wave function on the plane in the symmetric gauge with the same scaling of coordinates as above:

$$\Psi_\beta(z_1, \ldots, z_N) = Z_N^{-1/2}\prod_{i<j}(z_i - z_j)^\beta e^{-\frac{1}{2}\pi\beta\bar{\rho}\sum_i |z_i|^2}. \quad (24)$$

The droplet now achieves approximately uniform density $\bar{\rho}$ over a region on the plane bounded by the disk of radius $R = \sqrt{N/\pi\bar{\rho}}$. We can compute exactly the second moment of the density, using the following arguments. Under a rescaling of coordinates $z_i \to \lambda z_i$, the normalization integral is unchanged, which implies $\partial_\lambda \log Z_N(\lambda) = 0$. The derivative with respect to λ can then be carried out explicitly. The scaling of the

Laughlin-Jastrow factor, as well as the integration measure, produces a factor $\beta N(N-1)+2N$, while differentiation of the Gaussian exponential factor will result in the expectation value of $\sum_i |z_i|^2$. Then, setting $\lambda = 1$, we recover the exact sum rule:

$$\int |z|^2 \rho_\beta(z) d^2z = \frac{N}{2\pi\bar{\rho}}\left(N + \frac{2-\beta}{\beta}\right). \tag{25}$$

Subtracting off the density at $\beta = 1$, this becomes

$$\int |z|^2 (\rho_\beta(z) - \rho_1(z)) d^2z = \frac{N}{\pi\bar{\rho}}\left(\frac{1-\beta}{\beta}\right). \tag{26}$$

We are interested in the contribution to this sum rule that comes from the edge double layer. Consider a change of coordinates $r = R + y$, and take $R, N \to \infty$ while keeping $\bar{\rho}$ fixed. In this limit, we recover the edge density above as a function of y, the distance from the boundary. Now, we expand the left-hand side (LHS) of (26) in R, and use

$$2\pi \int_{-R}^{\infty} (R+y)[\rho_\beta(y) - \rho_1(y)] dy = 0, \tag{27}$$

which is just the statement that both densities ρ_β and ρ_1 count the same total number of particles. Dividing through by N and sending $R, N \to \infty$ then gives

$$\int_{-\infty}^{\infty} y[\rho_\beta(y) - \rho_1(y)] dy = -\frac{1}{4\pi}\left(\frac{\beta-1}{\beta}\right). \tag{28}$$

Thus the dipole moment is recovered and shown to be linear in $\nu - 1$. This explains the success of the perturbative expansion at order $\beta - 1$ in capturing the double layer.

VIII. EDGE DIPOLE MOMENT OF PFAFFIAN STATES

We can derive the same result for the Pfaffian states, defined by the ground-state wave function

$$\Psi_\beta^{pf} = \mathrm{Pf}\left(\frac{1}{z_i - z_j}\right) \Delta^\beta e^{-\frac{1}{2}\pi\beta\bar{\rho}\sum_i |z_i|^2}. \tag{29}$$

Here, $\mathrm{Pf}(M_{ij})$ is the Pfaffian of the matrix M [24]. Under this scaling, the Pfaffian states describing filling fraction $\nu = 1/\beta$ will have a mean density $\bar{\rho}$ in the bulk. For $\beta = 2$, this is the well-known Moore-Read state believed to describe the FQH effect at filling fraction $\nu = 5/2$. Following the arguments in the preceding section, we find the second moment of the density for the Pfaffian state:

$$\int |z|^2 \rho_\beta^{pf}(z) d^2z = \frac{N}{2\pi\bar{\rho}}\left(N + \frac{2-\mathcal{S}}{\beta}\right). \tag{30}$$

The quantity $\mathcal{S} = \beta + 1$ for Pfaffian states, and is known as the "shift" for FQH states. The shift relates the number of electrons in a FQH state needed to cover a sphere pierced by N_ϕ flux quanta, and is defined by the equation $N_\phi = \nu^{-1}N - \mathcal{S}$ [25]. Normalizability of the many-particle wave function on the sphere requires the holomorphic part of the wave function to be homogeneous of total degree $NN_\phi/2$. Comparing this with the total degree of the Pfaffian wave function $N(\beta N - \beta - 1)/2$ determines the shift [26], and accounts for its appearance in the second moment sum rule (30). Importantly, the shift determines the Lorentz shear modulus (odd viscosity) $\eta^{(A)} = \hbar\bar{\rho}\mathcal{S}/4$ [27]. Following the steps above, we deduce that the dipole moment for the Pfaffian state is, upon subtracting the $\beta = 1$ (free fermion) density for reference,

$$\int y\left[\rho_\beta^{pf}(y) - \rho_1(y)\right] dy = -\frac{1}{4\pi}\left(\frac{\mathcal{S}-2}{2\beta} + \frac{1}{2}\right). \tag{31}$$

Note that for Pfaffian states (29) with $\beta \geqslant 1$, the dipole moment is negative, indicating the presence of an overshoot at the edge. Furthermore, the dependence on $\mathcal{S}$, and not simply the filling fraction, confirms a connection between the strength of the dipole moment and the odd viscosity [11]. This connection is somewhat obscured in the Laughlin state for which $\mathcal{S} = \beta$.

While the result (31) is specific to Pfaffian states at filling fraction $\nu = \beta^{-1}$, it can be readily adapted to other FQH model wave functions. Indeed, the derivation requires that the ground state wave function in the symmetric gauge consists of a product of Gaussian exponential factors multiplied by a homogeneous function of particle coordinates of total degree $NN_\phi/2 = N(\nu^{-1}N - \mathcal{S})/2$. These are rather generic features of FQH model wave functions in the lowest Landau level, and suggest the dependence of the edge dipole moment (31) on the shift $\mathcal{S}$ is a general property of FQH states.

IX. CONCLUSION

In this paper, we studied the functional form of the edge density of the Laughlin state at filling fraction $\nu = \beta^{-1}$ using a perturbative expansion around the free fermion, IQH state at $\beta = 1$. From this we obtained the exact, finite N correction to the density at order $\beta - 1$. The correction becomes a universal function in the limit of large N, and we explicitly compute the odd moments and obtain exact asymptotics of the edge density. Our results confirm the presence of the dipole moment localized on the order of ℓ near the edge, which collapses to a singular double layer in the limit of large magnetic field. We have demonstrated that the perturbative result effectively captures the double layer structure of the edge, even for larger values of β, although it cannot account for the nonperturbative oscillatory features. Finally, we presented a route to analyze the edge structure of different FQH states, and derived the edge dipole moment of the Pfaffian state. The results reveal a relationship between the edge dipole moment and the bulk odd viscosity.

ACKNOWLEDGMENTS

P.W. and T.C. thank A. Abanov, A. Zabrodin, and I. Gruzberg for numerous discussions. The work of P.W. and T.C. was supported by NSF DMS-1206648, DMR-0820054 and BSF-2010345. P.W. thanks Andrea Cappelli for the hospitality at INFN Florence when this paper was completed. G.T. acknowledges financial support from Facultad de Ciencias, Uniandes.

[1] R. B. Laughlin, Phys. Rev. Lett. **50**, 1395 (1983).
[2] S. M. Girvin, A. H. MacDonald, and P. M. Platzman, Phys. Rev. B **33**, 2481 (1986).
[3] J. M. Caillol, D. Levesque, J. J. Weis, and J. P. Hansen, J. Stat. Phys. **28**, 325 (1982).
[4] A. nonmonotonic density profile is also seen in numerical studies of edge reconstruction D. B. Chklovskii, Phys. Rev. B **51**, 9895 (1995); L. Brey, *ibid.* **50**, 11861 (1994), where the edge breaks up into a number of different fractional states. This should not be confused with what we discuss in this paper, which is the universal features of the density profile of a FQH state at fixed filling fraction throughout.
[5] N. Datta, R. Morf, and R. Ferrari, Phys. Rev. B **53**, 10906 (1996).
[6] O. Ciftja and C. Wexler, Phys. Rev. B **67**, 075304 (2003).
[7] R. Morf and B. I. Halperin, Phys. Rev. B **33**, 2221 (1986).
[8] G. Téllez and P. J. Forrester, J. Stat. Phys. **97**, 489 (1999).
[9] P. Wiegmann, Phys. Rev. Lett. **108**, 206810 (2012).
[10] P. Wiegmann, JETP **117**, 538 (2013).
[11] F. D. M. Haldane, arXiv:0906.1854.
[12] S. M. Girvin and A. H. MacDonald, Phys. Rev. Lett. **58**, 1252 (1987).
[13] B. Jancovici, Phys. Rev. Lett. **46**, 386 (1981).
[14] A. Zabrodin and P. Wiegmann, J. Phys. A: Math. Gen. **39**, 8933 (2006).
[15] G. Téllez and P. J. Forrester, J. Stat. Phys **148**, 824 (2012).
[16] We used numerical data obtained through Monte Carlo techniques by A. Shytov for $N = 200$ particles.
[17] T. Can, P. J. Forrester, G. Téllez, and P. Wiegmann, arXiv:1310.3130.
[18] E. H. Rezayi and F. D. M. Haldane, Phys. Rev. B **50**, 17199 (1994).
[19] Ph. Choquard, P. J. Forrester, and E. R. Smith, J. Stat. Phys. **31**, 129 (1983).
[20] P. Wiegmann and A. Zabrodin (unpublished).
[21] L. Šamaj, J. Wagner, and P. Kalinay, J. Stat. Phys. **117**, 159 (2004).
[22] S. Jansen, E. H. Lieb, and R. Seiler, Commun. Math. Phys. **285**, 503 (2009).
[23] L. Šamaj and J. K. Percus, J. Stat. Phys. **80**, 811 (1995).
[24] G. Moore and N. Read, Nuc. Phys. B **360**, 362 (1991).
[25] X. G. Wen and A. Zee, Phys. Rev. Lett. **69**, 953 (1992); J. Fröhlich and U. M. Studer, Commun. Math. Phys. **148**, 553 (1992).
[26] N. Read and E. H. Rezayi, Phys. Rev. B **84**, 085316 (2011).
[27] N. Read, Phys. Rev. B **79**, 045308 (2009).